

1                   **A phylogenetic model for the recruitment of species into**  
2                   **microbial communities and application to studies of the**  
3                   **human microbiome**

4   **Running Title**

5   Phylogenetic community assembly of microbes

6  
7   **Authors**

8   John L. Darcy<sup>1</sup>, Alex D. Washburne<sup>2</sup>, Michael S. Robeson<sup>3</sup>, Tiffany Prest<sup>4</sup>, Steven K. Schmidt<sup>4</sup>, Catherine  
9   A. Lozupone<sup>1</sup>

10  
11   **Affiliations**

12   <sup>1</sup> Division of Biomedical Informatics and Personalized Medicine, University of Colorado School of Medicine,  
13   Aurora, Colorado, USA.

14   <sup>2</sup> Department of Microbiology and Immunology, Montana State University. Bozeman, Montana, 59717,  
15   USA.

16   <sup>3</sup> Department of Biomedical Informatics, University of Arkansas for Medical Sciences. Little Rock, Arkansas,  
17   72205, USA.

18   <sup>4</sup> Department of Ecology and Evolutionary Biology, University of Colorado. Boulder, Colorado, 80309,  
19   USA.

20  
21   **Corresponding Author**

22   J.L. Darcy; darcyj@colorado.edu.

23  
24   **Conflict of Interest Statement**

25   The authors declare that no conflict of interest exists.

26  
27   **Support**

28   Funding was provided by an NSF grant for studying microbial community assembly following disturbance  
29   (DEB-1258160) and by a NIH NLM Computational Biology training grant (5 T15 LM009451-12). The fund-  
30   ing bodies had no role in study design, analysis, interpretation, or in the preparation of this manuscript.  
31

## 32 Abstract

33 Understanding when and why new species are recruited into microbial communities is a formidable prob-  
34 lem. Much theory in microbial temporal dynamics is focused on how phylogenetic relationships between  
35 microbes impact the order in which those microbes are recruited; for example species that are closely re-  
36 lated may exclude each other due to high niche overlap. However, several recent human microbiome studies  
37 have instead found that close phylogenetic relatives are often detected in microbial communities in short  
38 succession, suggesting factors such as shared adaptation to similar environments play a stronger role than  
39 competition. To address this, we developed a mathematical model that describes the probabilities of dif-  
40 ferent species being detected in time-series microbiome data, within a phylogenetic framework. We use our  
41 model to test three hypothetical assembly modes: underdispersion (species are more likely to be detected if a  
42 close relative was previously detected), overdispersion (likelihood of detection is higher if a close relative has  
43 not been previously detected), and the neutral model (likelihood of detection is not related to phylogenetic  
44 relationships among species). We applied our model to longitudinal high-throughput sequencing data from  
45 the human microbiome, and found that for the individuals we analyzed, the human microbiome generally  
46 follows an assembly pattern characterized by phylogenetic underdispersion (*i.e.* nepotism). Exceptions were  
47 oral communities, which were not significantly different from the neutral model in either of two individuals  
48 analyzed, and the fecal communities of two infants that had undergone heavy antibiotic treatment. None of  
49 the datasets we analyzed showed statistically significant phylogenetic overdispersion.

## 51 Introduction

52 Every non-sterile surface in the world is in some stage of community assembly, from a forest of tropical  
53 trees to the microbes in a mammalian gut. The communities of organisms inhabiting these environments are  
54 dynamic through time, and studying patterns of assembly may shine light on general rules that govern their  
55 change. Understanding these community assembly rules may aid habitat restoration [1; 2], the management  
56 of ecosystems that have undergone disturbances [3; 4], and ecological theory of community phylogenetics  
57 [5; 6]. Patterns and rules of community assembly are particularly important in human systems, including the  
58 primary succession of microbes on a human host following birth [7], secondary successions following disease  
59 [8; 9], disturbances caused by host lifestyle or antibiotic use [10; 11; 12], and the natural turnover of microbial  
60 communities over time [13]. Insights into these difficult-to-observe community assembly processes can be  
61 gained via the comparison of microbial communities using high-throughput DNA sequencing [13; 14; 15],  
62 especially in longitudinal (time-series) studies [13; 7; 11].

63 A central question in microbial community assembly is when and why microbes are recruited into com-  
64 munities. The empirical detection of new species can be studied by evaluating the order in which species are  
65 detected in time-series experiments, given data such as which species have already been detected or what  
66 changes occur in an environment over time [14; 16]. Although a changing environment clearly selects for  
67 new species, it has also been shown that microbial community structure is often historically contingent on  
68 previous states of that community [14; 17; 16; 18; 19]. This reflects not only that microbial communities are  
69 temporally autocorrelated (gradual change over time), but also that the recruitment of a given species is a  
70 function of which species in the community are already present or have modified the local environment. Such  
71 historically contingent patterns have mainly been observed and tested within a phylogenetic context, because  
72 amplicon data naturally lend themselves to the creation of phylogenies, and because phylogenies have been  
73 shown to be predictive of genomic (and perhaps niche) overlap in human associated microbiota [20; 21].

74 Within this phylogenetic framework, a predominant hypothesis has been that closely related microbes  
75 inhibit each other's successful recruitment [14; 17; 18]. The proposed mechanism for this hypothesis is that  
76 closely related microbes likely have similar niches (phylogenetic niche conservatism [22]), and species already  
77 established within a community will occupy their niches to the exclusion of ecologically similar strains.  
78 This is also the basis of Darwin's naturalization hypothesis [23], which proposed that new species are less  
79 likely to be recruited if a close relative is present [24]. Indeed, this assembly mode has been found to  
80 be the case in artificial nectar microcosms, where phylogenetically similar yeast species had similar nutrient  
81 requirements, and inhibited each others' colonization [25]. In this paper, we refer to the assembly mode where  
82 distant relatives are more likely to be recruited into a community than close relatives as the **overdispersion**  
83 **hypothesis**, since it predicts the preferential addition of novel phylogenetic diversity to a community (*i.e.*

84 phylogenetic overdispersion).

85 Overdispersion is far from universal, and multiple studies have shown that extremely close relatives can  
86 coexist within the human microbiome [26; 27; 28], and may even be preferentially recruited [29]. This is  
87 consistent with simulations showing that clusters of closely-related species can persist despite strong within-  
88 cluster competition, when immigration rate is high [30]. Indeed, Darwin’s pre-adaptation hypothesis predicts  
89 that species with a close relative present in a community will be preferentially recruited, because they are  
90 likely to already be adapted to the new environment [23]. This hypothesis predicts that new close relatives  
91 are more likely to be detected than new distant relatives, so the amount of new phylogenetic diversity added  
92 to a community is minimized (phylogenetic underdispersion). For this reason, we refer to this hypothesis  
93 as the **underdispersion hypothesis**. The over- and underdispersion hypotheses are alternatives to the  
94 null hypothesis that recruitment is independent of phylogenetic relatedness among species. Since the null  
95 hypothesis is species-neutral (and phylogenetically neutral), we refer to it as the **neutral hypothesis**.

96 It should be noted that our use of the terms “overdispersion” and “underdispersion” are slightly different  
97 in this manuscript compared to use of the same terms elsewhere. In many cases, these words refer to the  
98 state of a community at a single timepoint or sample, with overdispersion indicating more diversity in that  
99 sample than expected by chance, and underdispersion indicating less [31]. Instead, our use of over- and  
100 underdispersion refers to the amount of newly added diversity over time. In our overdispersion hypothesis,  
101 phylogenetically novel species are preferentially added to communities, meaning more new diversity is added  
102 than expected by chance. Under our underdispersion hypothesis, the reverse is true. Following this, our  
103 question concerns the order in which new species are detected in a time-series, rather than community  
104 composition of any given sample.

105 Here, we use the phylogenetic relationships among species within a time-series to test the extent to which  
106 our over- or underdispersion hypotheses hold true. Instead of analyzing broad patterns of community change  
107 via beta-diversity statistics (*e.g.* UniFrac [32]) or analyzing patterns of select clades within the community  
108 (*e.g.* PhyloFactor [33], Edge PCA [34]), we model the probability of detecting new species in a community  
109 for the first time as a monotonic function of their phylogenetic distances to members of the community that  
110 have already been detected.

111 The model we present here can be used to estimate the degree to which the detection of new species is  
112 more or less likely when a close relative is already present, using empirical data. We fit our model to several  
113 time-series human microbiome datasets [13; 7; 35] to compare the strength of under- or overdispersion be-  
114 tween subjects, sample sites, or time periods. We found that for the data sets we analyzed (36 individuals  
115 across 3 studies), the human microbiome generally follows the underdispersion hypothesis. There were excep-  
116 tions where this pattern was not significantly different than the neutral model, but none of the longitudinal  
117 datasets we analyzed showed statistically significant overdispersion.

118

## 119 Materials and Methods

### 120 Overview

121 With our model, our goal is to estimate the extent to which detection of new species over time is related to  
122 the new species’ phylogenetic similarity to (or distance from) species that were already detected at previous  
123 timepoints. Our **Statistical Model** describes the probabilities of detecting new species over time. We  
124 use our model with empirical data via **Simulations**, where we re-sample the empirically detected species  
125 using our model with known parameter values, to produce surrogate datasets. Specifically, we fix and record  
126 the model’s dispersion parameter ( $D$ ), which determines the extent to which species with a close relative  
127 are preferentially added to the surrogate community (or, conversely, if species without a close relative are  
128 preferred). Our **Parameter Estimation** compares the empirical pattern of species detection to that of the  
129 surrogate datasets (which have known  $D$  values), in order to determine which value of  $D$  best describes the  
130 empirical data. **Hypothesis Testing** is done by comparing empirical data to repeated simulations under  
131 the neutral model, which is  $D = 0$ . We describe the bioinformatic and technical details of this process in our  
132 **Analysis** section, and make our code available to others in the **Code and Data** section.

## 133 Statistical Model

134 At any point in time, a community is composed of many species, and other species are not present but  
135 are available to be added ("species pool"). Our model parameterizes the probability of detecting species in  
136 a local community for the first time, based on their phylogenetic distances from species that have already  
137 been detected. In a species-neutral model of community assembly, each species  $i$  in the species pool has the  
138 same probability of detection at time  $t$ , irrespective of how different it is from species that have already been  
139 detected. Thus, the neutral model for first-time species detections is a random draw without replacement of  
140 species from the species pool. We extend the species-neutral model by modeling the probability  $p_{it}$  of species  
141  $i$  being detected for the first time at time  $t$  as,

$$p_{it} = \frac{d_{it}^D}{\sum_i d_{it}^D} \quad (1)$$

142 where  $d_{it}$  is the phylogenetic distance from species  $i$  to its closest relative that has already been detected  
143 prior to timepoint  $t$ , and  $D$  is a dispersion parameter.

144 When  $D = 0$ , our model functions as a neutral model; all species have the same probability of being  
145 detected for the first time, since  $p_{it}$  is the same for every species. When  $D < 0$ ,  $p_{it}$  decreases with  $d_{it}$   
146 meaning that species from the species pool have higher probabilities of detection when they are more closely  
147 related to species that have already been detected in the local community (underdispersion; phylogenetically  
148 constrained). When  $D > 0$ , the opposite is true (overdispersion; phylogenetically divergent). Our hypothesis  
149 testing and parameter estimation focus on the dispersion parameter,  $D$ .

## 150 Simulations

151 Our analysis of a dataset relies on re-constructing that dataset via simulation of our statistical model  
152 using known values of  $\hat{D}$ , allowing for hypothesis testing and parameter estimation (we refer to the empirical  
153 dispersion parameter as  $D$ , and use  $\hat{D}$  to refer to surrogate values used in simulations). Using the empirical  
154 data as a starting point, we simulate many surrogate datasets with  $\hat{D}$  values ranging from  $\hat{D} < 0$  (underdis-  
155 persed) to  $\hat{D} = 0$  (neutral) to  $\hat{D} > 0$  (overdispersed). This is done so that the empirical data can later be  
156 compared to the surrogate datasets, to estimate the empirical value of  $D$ .

157 We start each surrogate dataset with the same species present in the first sample in the time-series of  
158 its corresponding empirical dataset. Then, surrogate datasets are constructed forward in time by randomly  
159 drawing  $r_t$  new species from the species pool, where the probabilities of detecting those species are given by  
160 Equation 1, and  $r_t$  is the number of new species detected in the empirical dataset from times  $t - 1$  to  $t$ . The  
161 number of new species detected from the empirical dataset is used so that species richness is kept constant  
162 between the empirical dataset and all surrogate datasets. The species pool is updated to exclude those  
163 species drawn at previous timepoints, and the newly sampled species are recorded. Surrogate datasets are  
164 produced for many different  $\hat{D}$  values, ranging from underdispersed to overdispersed models. We performed  
165 500 simulations (as described above) for each dataset analyzed.

## 166 Parameter Estimation

167 Our main goal is to estimate the empirical dispersion parameter  $D$  (Equation 1), which quantifies the  
168 degree to which first-time species detections are phylogenetically underdispersed ( $D < 0$ ), neutral ( $D = 0$ ),  
169 or overdispersed ( $D > 0$ ), corresponding to our hypotheses. To this end, we use Faith's phylogeny [36]  
170 to compare each of the 500 surrogate datasets (described above) to the empirical dataset. Phylogeny  
171 is the sum of branch-lengths on a phylogenetic tree for a set of species, so phylogeny of a set of highly  
172 related species is low (phylogenetically constrained) because there are no long branch lengths in the tree, but  
173 phylogeny is higher (phylogenetically divergent) for a set of more distantly related species [36]. If  $D \neq 0$ ,  
174 then species are preferentially added if they have relatively low ( $D < 0$ ) or relatively high ( $D > 0$ ) phylogenetic  
175 distance to the resident community ( $d_{it}$ , Equation 1), yielding accumulations of total phylogeny that are  
176 relatively slow ( $D < 0$ ) or relatively fast ( $D > 0$ ) compared to the neutral model (Fig. 1A). In other words,  
177 at any timepoint  $t$ , the phylogenetic diversity of species that have already been observed is  $PD_t$ , and the  
178 extent to which  $PD_t$  accelerates or decelerates over a sampling effort depends on  $D$ . Because of this, we can

179 estimate  $D$  by comparing the empirical phylodiversity curve to our surrogate phylodiversity curves, which  
180 have known  $\hat{D}$  values.

181 For the comparison of an empirical phylodiversity accumulation curve to curves for corresponding sur-  
182rogate datasets, we evaluate the amount of phylodiversity  $PD_m$  accumulated at time index  $m$ , midpoint  
183 between the first and final samples. Time  $m$  is used because this leaves many species yet to be observed in  
184 the species pool, so that there can be variability in surrogate datasets. Multiple time indices are not used to  
185 compare surrogate and empirical datasets because each value  $PD_{\hat{t}}$  is a function of all values  $PD_{t < \hat{t}}$ .  $PD_m$   
186 values are calculated for all surrogate datasets, and a  $PD_m$  value is calculated for the empirical dataset.  
187 The difference between the empirical  $PD_m$  and  $PD_m$  simulated with  $D = \hat{D}$  is  $\Delta PD_{\hat{D}}$ , which is the error  
188 between surrogate and empirical data. We then estimate the empirical value of  $D$  by minimizing  $\Delta PD_{\hat{D}}$   
189 (Fig. 1B). This minimization is performed using a logistic error model,

$$\Delta PD_{\hat{D}} = \frac{a - b}{1 + e^{-r(\hat{D} - i)}} + b \quad (2)$$

190 where  $a$  and  $b$  are the upper and lower horizontal asymptotes, and  $r$  and  $i$  are rate and inflection parameters  
191 for the logistic model.  $\Delta PD_{\hat{D}}$  is modeled with a logistic function because there is a maximum and minimum  
192 observable  $\Delta PD_{\hat{D}}$  value as a function of the phylogeny; this is because there are strict minimum and maximum  
193 limits to the amount of phylodiversity obtainable by observing  $n$  species where  $n$  is the total species richness  
194 accumulated up to time  $m$ . The two horizontal asymptotes of the logistic model are easily fit to these  
195 extremes (Fig. 1B). Once fit, the error model is solved for  $\Delta PD = 0$ , giving an estimate for the empirical  
196  $D$ . Confidence intervals for this estimate are obtained via bootstrapping our error model.

## 197 Hypothesis Testing

198 For this test, our null hypothesis is the neutral model, where  $D = 0$ , since this model represents the  
199 absence of the effect we are testing. We test this null hypothesis competitively by simulating 1000 surrogate  
200 datasets at  $D = 0$  (Fig. S1A) to generate a null  $PD_m$  distribution. The empirical  $PD_m$  is compared to this  
201 distribution (Fig. S1B), and if the empirical  $PD_m$  is below the 2.5% quantile or above the 97.5% quantile,  
202 we reject the null (*i.e.* neutral) hypothesis. Evidence of either overdispersion ( $D > 0$ ) or underdispersion  
203 ( $D < 0$ ) allows us to reject.

## 204 Analysis

205 This section is a summary of our data analysis. Detailed methods for this section are available as supple-  
206 mental information.

207 We ran our model on data from 36 individuals from three data sources. Two individuals were from  
208 Caporaso *et al.* [13], 33 were from Yassour *et al.* [35], and one was from Koenig *et al.* [7]. In all cases,  
209 data were downloaded and processed using the unoise3 pipeline [37], which clusters sequence data into exact  
210 sequence variants called zOTUs. The Koenig *et al.* infant gut data set was split into two data sets, one for  
211 samples collected before the subject began consuming baby formula, and one after. Our model was run on  
212 these data as described above, resulting in  $D$  estimates for the before and after formula data sets.

213 The “moving pictures” [13] data were split into eight datasets, one for each combination of subject ( $n=2$ )  
214 and body site (feces, right and left palms, tongue), and our model was run on each of these datasets. Analyses  
215 of these data was also done using two approaches that allowed us to test the importance of the set of species  
216 that are included in the species pool. One alternate approach analyzed communities in a “meta” context,  
217 where the species pool for a given palm was composed of all four palms in the whole dataset. If we were  
218 to estimate similar  $D$  values for both the “meta” and “self” analyses, the inclusion of extra species in the  
219 species pool would be of little importance to the model. The other alternate approach analyzed data using  
220 a sliding-window approach, wherein our model was run separately on multiple overlapping windows of 5  
221 consecutive days within the same dataset, in order to see how  $D$  varied over time.

222 Finnish infant sequence data from Yassour *et al.* [35] were split into data sets for each of 33 individuals,  
223 and our model was run for each. Estimated  $D$  values were compared between subjects that had been treated  
224 with oral antibiotics ( $n=18$ ) and subjects that had not ( $n=15$ ) using a Mann-Whitney test. Because this data  
225 source had so many subjects, we used these data to test whether the number of zOTUs, total phylodiversity,  
226 or number of timepoints had an effect on  $D$  estimates via correlation analysis.

## 227 Code and Data

228 R code and data to replicate our analysis, or to perform a similar analysis on other data, are available on  
229 GitHub, at [https://github.com/darcyj/pd\\_model](https://github.com/darcyj/pd_model).

## 230 Results

231 By varying  $\hat{D}$ , we successfully changed the rate at which phylodiversity is added to surrogate (*i.e.* re-  
232 sampled) microbial communities over time (Fig. 1A). Compared to the neutral model where  $\hat{D} = 0$ , higher  
233  $\hat{D}$  values result in phylodiversity accumulating quickly, since in the overdispersed model, species that con-  
234 tribute more phylodiversity are preferentially sampled. Conversely, lower  $\hat{D}$  values result in phylodiversity  
235 accumulating slowly, since in the underdispersed model, species that contribute less phylodiversity (since  
236 they are very similar to species that are already present) are preferentially sampled. These results show that  
237 the  $D$  parameter in our model successfully corresponds to over- and underdispersion relative to the neutral  
238 model. Our error model also fit well to the differences between empirical and surrogate datasets ( $\Delta PD_{\hat{D}}$ ,  
239 Fig. 1B). Each error model fit was visually inspected for goodness of fit, to be sure that  $D$  estimates were  
240 not spurious. All data sets passed this inspection.

### 241 Results from “moving pictures” data

242 All time-series from adult feces and palm microbiomes [13] showed significant phylogenetic underdispersion  
243 of first-time zOTU detections (Fig. 2). This means that when a zOTU was detected for the first time in one  
244 of these communities, it was more likely to be phylogenetically similar to a zOTU that had previously been  
245 detected in community. For both the male and female subject,  $D$  estimates were lower (more underdispersed)  
246 in the feces than in the palms, left and right palm  $D$  estimates were similar to each other, and tongue  $D$   
247 estimates were higher. All sites except the tongue showed statistically significant underdispersion in both  
248 subjects, while tongue data were not significantly different than the neutral model. In the comparison between  
249 “meta” and “self” models, “meta” models needed to be much more underdispersed than “self” in order to  
250 approximate empirical phylogenetic diversity accumulation (Fig. S2). We also observed a general upward  
251 trend in  $D$  in our sliding window analysis of the male right palm dataset (Fig. S3), although this trend was  
252 only observed over 19 days.

### 253 Results from infant gut data

254 Empirical phylodiversity accumulation in the infant gut microbiome [7] showed a sharp increase in phy-  
255 lodiversity after day 161 (Fig. 3), the same date that the subject began consuming baby formula. This  
256 suggests that baby formula changed the phylogenetic colonization patterns of the developing infant gut. We  
257 analyzed this dataset as two separate time-series, one before formula use and one during, and both had  
258 negative  $D$  estimates, with the pre-formula  $D$  estimate being lower (Fig. 4). While the pre-formula dataset  
259 was significantly underdispersed ( $P = 0.007$ ), the formula dataset was not significantly different from the  
260 neutral model, although this result is marginal ( $P = 0.107$ ). Infant gut data from Finnish infants [35] were  
261 sampled at a much lower temporal resolution, and as such were not split between formula use. 31 out of 33  
262 individuals analyzed exhibited significant underdispersion, and the other two were not significantly different  
263 from the neutral model. Both nonsignificant individuals were from the group treated with heavy antibiotics,  
264 but even so, no significant difference in  $D$  values was detected between antibiotics and control groups (Fig.  
265 S4). Estimates of  $D$  did not significantly correlate with the number of zOTUs in a dataset, the total phylo-  
266 diversity of the dataset, the initial phylodiversity of the dataset, or the number of samples in a dataset (Fig.  
267 S5).

## 268 Discussion

269 Any organism of interest in a human microbiome dataset, from the pathogenic to the probiotic, will at  
270 some point be detected for the first time, and the order in which these organisms are detected in the com-  
271 munity is determined by community assembly processes [14]. Predicting which lineages of organisms can be

272 recruited into a given environment has far-reaching implications for ecosystem remediation and management,  
273 especially in microbial communities where the medical and ecological importances of many microbes are still  
274 largely unknown [38; 39]. Identifying conditions under which assembly mechanisms change, or under which  
275 non-neutral assembly is particularly strong, may facilitate microbial community rehabilitation by understand-  
276 ing when and how microbial communities can be colonized by close/distant relatives. If there are patterns or  
277 general rules for which taxa have higher probabilities of recruitment, these rules can guide habitat restora-  
278 tion projects, help us better design probiotics for colonization, and better exploit disturbance as a tool for  
279 managing microbial systems related to human health and disease. We found that assembly during primary  
280 succession of the infant gut (Fig. 4, Fig. S4) and during turnover of the microbial communities on the adult  
281 palms and gut (Fig. 2) follows a predictable pattern: new species are more likely to be detected if a close  
282 relative has been detected previously.

283 We describe new species appearing as "detections" because of the difference between empirical data  
284 and actual phenomena. Species recruitment into communities is a phenomenon under investigation in our  
285 model, but evidence for recruitment is a lack of detection, and then subsequent detection of a species using  
286 high-throughput DNA sequencing data. With such data, it is possible for a species to have been recruited  
287 into a community but not be detected, although this source of experimental error diminishes as sequencing  
288 depth increases. Furthermore, the extent to which a species has actually been recruited into a community  
289 is questionable, if it is sufficiently rare that it is not detected in an Illumina sequencing run with tens of  
290 thousands of reads per sample (*e.g.* [35]). Future work may use techniques such as qPCR to quantify  
291 abundances of individual species or strains [40], and exclude those that do not meet an *a priori* abundance  
292 threshold for detection. Nevertheless, in order to be conservative in our language and our approach, we  
293 have described our model and our hypotheses in terms of modeling the detection of new species, rather than  
294 modeling their recruitment.

295 The generally "nepotistic" pattern we observed in new species detection supports our underdispersion  
296 hypothesis, which follows Darwin's pre-adaptation hypothesis [23] and more recent ecological theory as well  
297 [30; 41]. Much work in phylogenetic community ecology posits that competition tends to be strongest among  
298 closely-related species due to phylogenetic niche conservatism [42], so many closely-related species are able  
299 to coexist in a community, competition must not be an important factor structuring that community [31].  
300 However, strong competition between distantly related species may actually cause groups of phylogenetically  
301 similar species to coexist, especially when immigration is high [30; 41; 43]. This type of competition is perhaps  
302 better conceptualized as environmental filtering instead [41], especially since studies showing evidence for  
303 competitive exclusion in microbial communities focus on competition between closely-related species [25; 16].

304 our model investigates the extent to which newly detected species are likely to be similar to previously  
305 detected close relatives, but "previously detected" may include a significant time span. Thus, the observation  
306 of underdispersion may not reflect a lack of importance of competition *per se*. However, testing whether new  
307 species detections are likely after a close relative has already been detected has relevance; for instance in  
308 human microbiome systems it may be beneficial to understand if a pathogen's probability of detection may  
309 be higher if a conspecific strain was previously observed [26; 28]. Approaches that consider only recent  
310 community membership may more directly inform hypotheses regarding direct competition, or regarding  
311 more recent detection of close relatives. For this reason, we included a sliding-window analysis of 5-day  
312 intervals for a subset of intensively-sampled data, and showed significant underdispersion in a majority of  
313 windows analyzed (Fig. S3). This type of analysis can satisfy the issue of recency when using our model,  
314 but only when data collection is sufficiently frequent.

315 Regardless, non-neutral patterns of phylogenetic community structure have been interpreted to mean that  
316 traits are under ecological selection [44; 31; 45; 46]. If traits are not driving community assembly [47] or if  
317 the traits driving community assembly are largely horizontally transferred between taxa independent of their  
318 relatedness (as estimated by a 16S rDNA phylogeny), we would expect no phylogenetic signature, and a  $D$   
319 estimate that is not significantly different from 0 (the neutral model). Instead, we observed a very strong  
320 and significant phylogenetic signal in species detection order for almost all datasets we analyzed. However,  
321 if selection on traits is driving this pattern, selection itself may not occur within the host environment. An  
322 alternative explanation for the underdispersion we observed is that selection is external to the host envi-  
323 ronment (*i.e.* selection occurs within the neighboring species pool from which emigration occurs), causing  
324 change in the community entering the host to already be underdispersed. Similarly, phylogenetic dispersion  
325 of community structure has been unable to distinguish between selection and differences in migration rates

[48], so a pre-underdispersed community entering the host is a plausible mechanism for phylogenetic underdispersion of species detection. But selection of microbial communities within the host has been shown by multiple studies [10; 9; 11], so it is our opinion that selection within the host is a more likely scenario.

As to why no datasets analyzed showed significant phylogenetic overdispersion ( $D > 0$ ), we are not certain. At the beginning of development of this model, we expected microbial communities in the human microbiome to follow the overdispersion hypothesis, partly from microbiome studies suggesting competition among closely-related bacteria is an important factor in human gut microbial community assembly [49; 50], and also because of work in experimental microcosms [25]. However, the human microbiome environments analyzed here are environments that undergo constant physical disturbance, unlike aqueous microcosms. Palm communities are physically disturbed with every use of the hands, and by the sampling procedure itself. Gut (fecal) communities are also disturbed constantly by the movement of feces through the gut. It may be possible that continuous disturbance allows for underdispersion via constant re-assembly of communities. In this case, niches may be filled by random “winners” after each disturbance, as in a competitive lottery scenario [18]. These “winners” would still need to be pre-adapted to their environment, so they would be more likely to be closely related to previous “winners”, as in our findings. Similarly, environments with fluctuating resource profiles may result in clusters of organisms occupying the same niche [51]. The datasets we used are also somewhat limited in terms of phylogenetic resolution, as short reads of the 16S marker gene are insufficient to detect strain-level variation [52; 50; 27]. Thus, competitive exclusion could occur at the extreme tips of the bacterial phylogenetic tree, and this would not be detectable using 16S rDNA data. Even so, broader patterns of underdispersion at phylogenetic depths accessible with 16S data could still result in significantly underdispersed model fits.

A strength of our model is that it estimates values of  $D$  that can be compared among datasets (Fig. 2) or potentially across time (Fig. 4, Fig. S3) in order to learn how differences between datasets impact community assembly. We found that gut and palm communities were almost universally underdispersed (Fig. 2, Fig. 4, Fig. S4), and that the  $D$  value for a community appears to be a function of body site (Fig. 2). Although this result is only shown across two subjects, the parallel patterns between the male and female subject are striking, in that fecal communities are the most strongly underdispersed (lowest  $D$ ), palm communities are similar to each other, and tongue communities had the highest  $D$  estimates. Similarly, comparing  $D$  before and after an event can be used within an experimental framework to see how that event may affect community assembly. Our analysis of infant gut microbiome data [7] before and during the use of baby formula (Fig. 4) showed that while the pre-formula community was significantly underdispersed, community assembly during formula consumption was more neutral. While the post-formula trend was not significantly different from the neutral model, this finding was marginal ( $P = 0.107$ ).

In addition to showing that our model can be a useful tool for future studies, our findings also hint that phylogenetic underdispersion may be a common trend for the human gut microbiome, although demonstrating a general trend would require analysis of more than the 36 individuals we analyzed. Indeed, recent research has shown that for fecal transplants, donor strains are able to integrate into the recipient’s gut community when a conspecific strain is already present, but novel donor strains are unlikely to successfully integrate into the recipient [26]. Congeneric bacteria have also been shown to be predictors of each others’ recruitment in the mouse gut microbiome, both for pathogens and commensals [28]. Different body sites - as we saw with the skin - may have qualitatively similar patterns of underdispersion, yet quantitatively different magnitudes of this effect. Thus the efficacy of an engineered probiotic based on similarity to organisms already present in the community for which it was engineered may largely depend on the body site for which it’s intended, although again more exhaustive study is needed. To facilitate further discovery both in the human microbiome and in other environments, we have made our R code and a tutorial available on GitHub: [https://github.com/darcyj/pd\\_model](https://github.com/darcyj/pd_model).

## Acknowledgements

The authors thank D.R. Nemergut for her help and support, and also thank P. Sommers, E. Gendron, A. Solon, E. Pruesse, A. Armstrong, C. Martin, K. Hazleton, and S. Sauce for many helpful discussions. Funding was provided by an NSF grant for studying microbial community assembly following disturbance (DEB-1258160) and by a NIH NLM Computational Biology training grant (5 T15 LM009451-12).

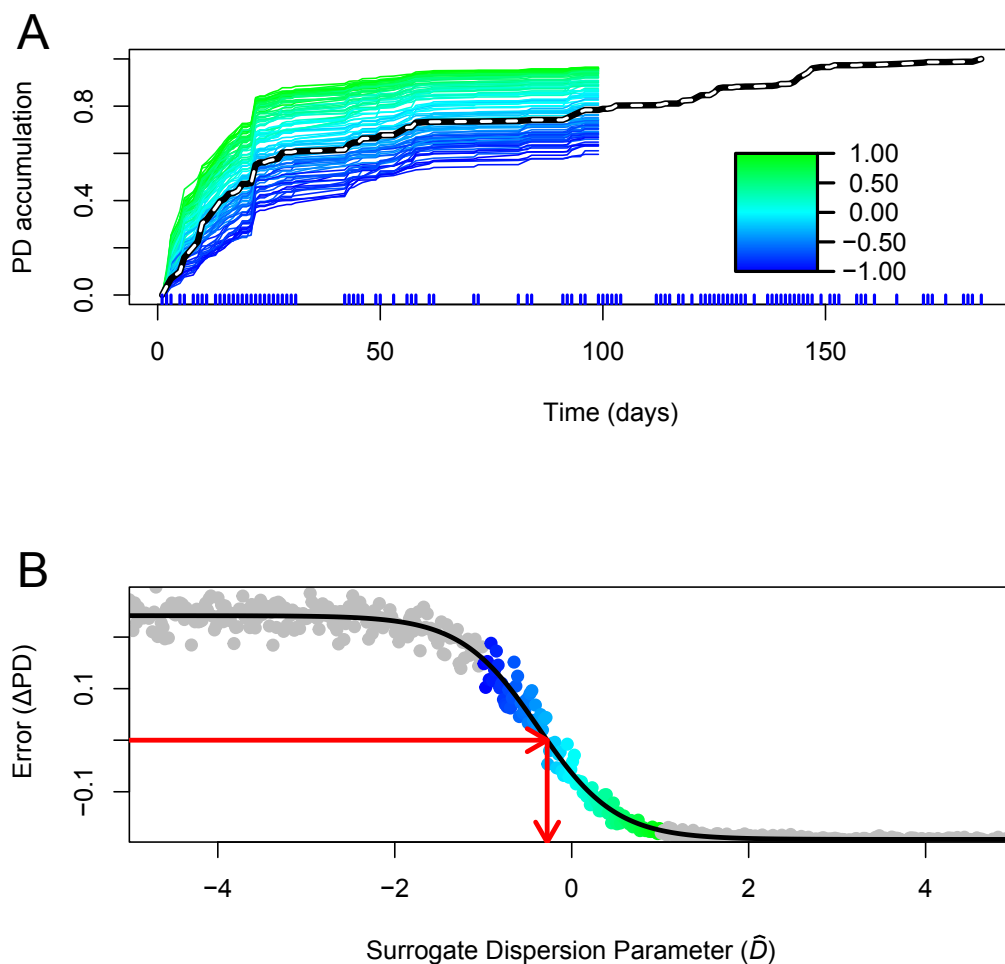


## <sup>377</sup> **Conflict of Interest**

<sup>378</sup> The authors declare that no conflict of interest exists.

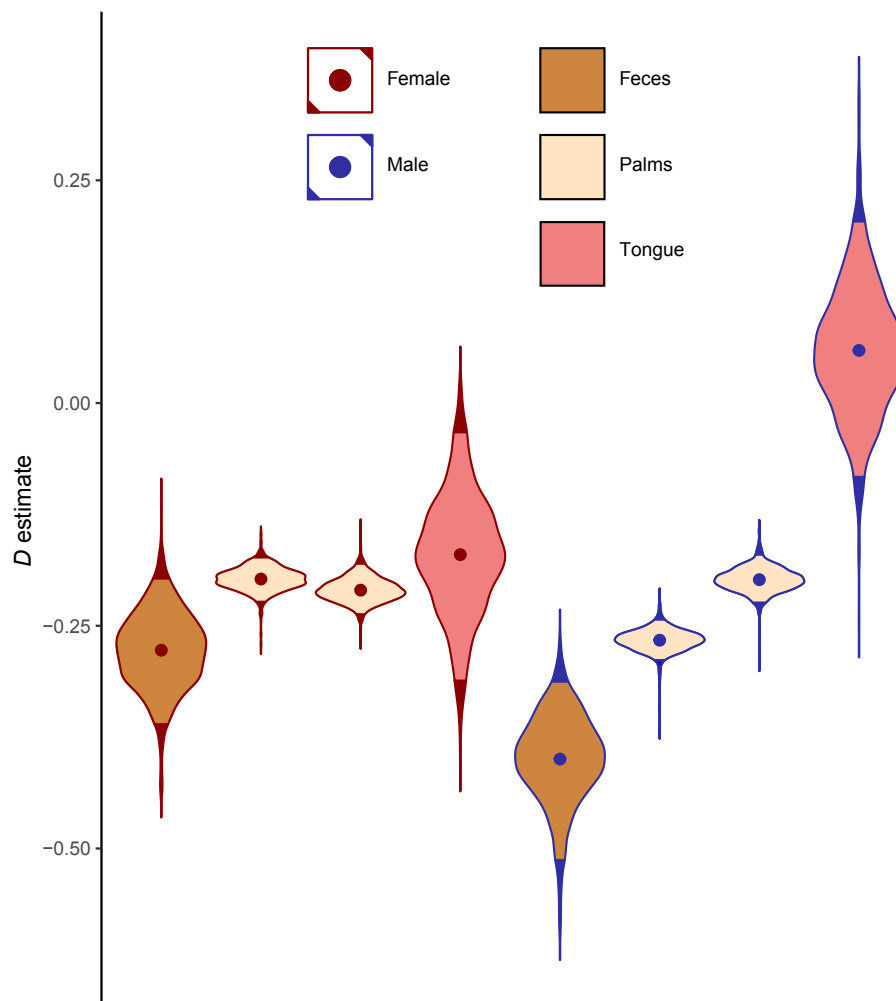
379 **Figures**

380 **Fig. 1**



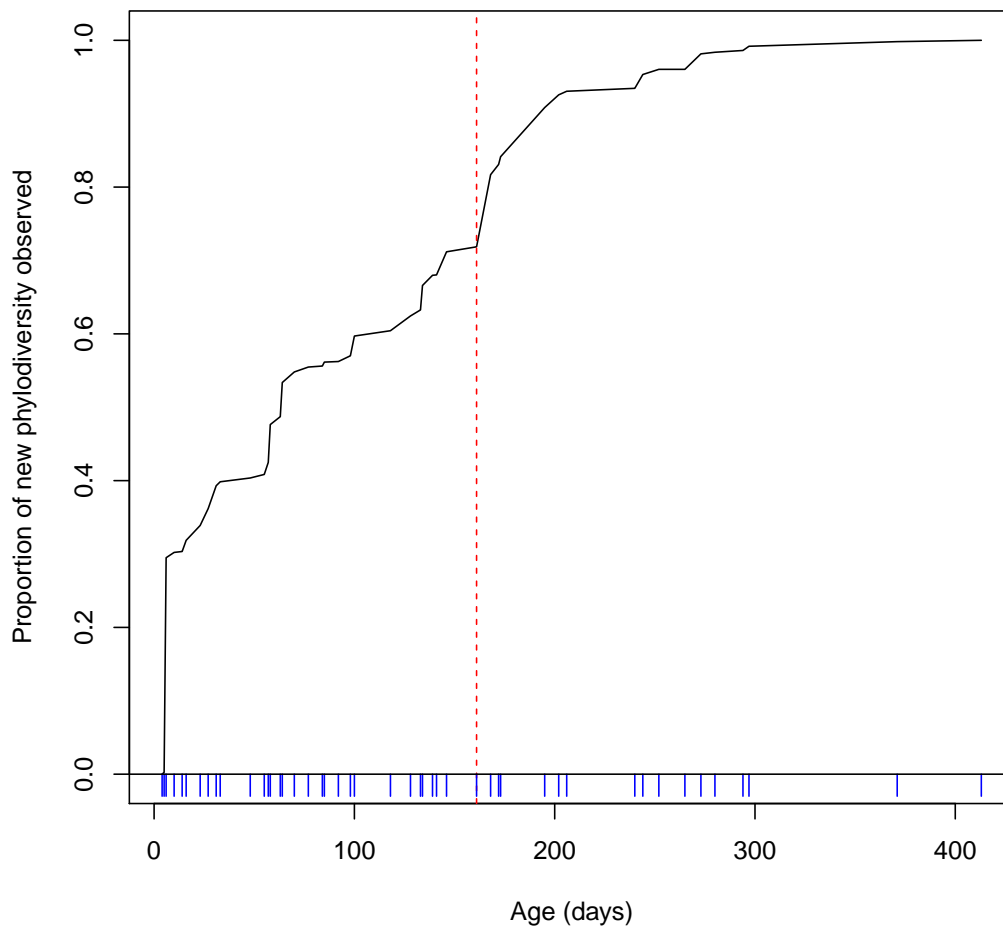
381 Phylogenetic diversity accumulation and model fitting in the female feces dataset [13]. Plot A shows empirical  
382 (dashed) and surrogate phylogenetic diversity accumulation curves. Surrogate curves are colored according to  $\hat{D}$   
383 value (Equation 1). New species that have a previously-detected close relative contribute little phylogenetic diversity  
384 and cause slow phylogenetic diversity accumulation (blue). New species that do not have a close relative contribute  
385 more phylogenetic diversity and cause faster accumulation (green). The empirical model (dashed) is below the neutral  
386 model (teal), signifying underdispersion in the order of first-time species detections. The times of sampling  
387 points are shown as vertical blue lines below the X-axis. Curves are rescaled from 0 to 1 in this figure.  
388 Plot B shows how empirical and surrogate data are compared to generate an estimate for  $D$ . Differences  
389 between empirical and surrogate data at time  $m$  are shown on the Y-axis, and the  $\hat{D}$  values used to generate  
390 surrogate datasets are shown on the X-axis. Color-coded points correspond to surrogate datasets shown in  
391 plot A. Values shown in gray result from using extreme values of  $\hat{D}$ , which help the logistic error model (black  
392 line) fit to the data, and are not shown in plot A. The red arrows show the process of error minimization,  
393 yielding a  $D$  estimate. A figure showing significance testing for these data is available as Fig. S1.

394 **Fig. 2**



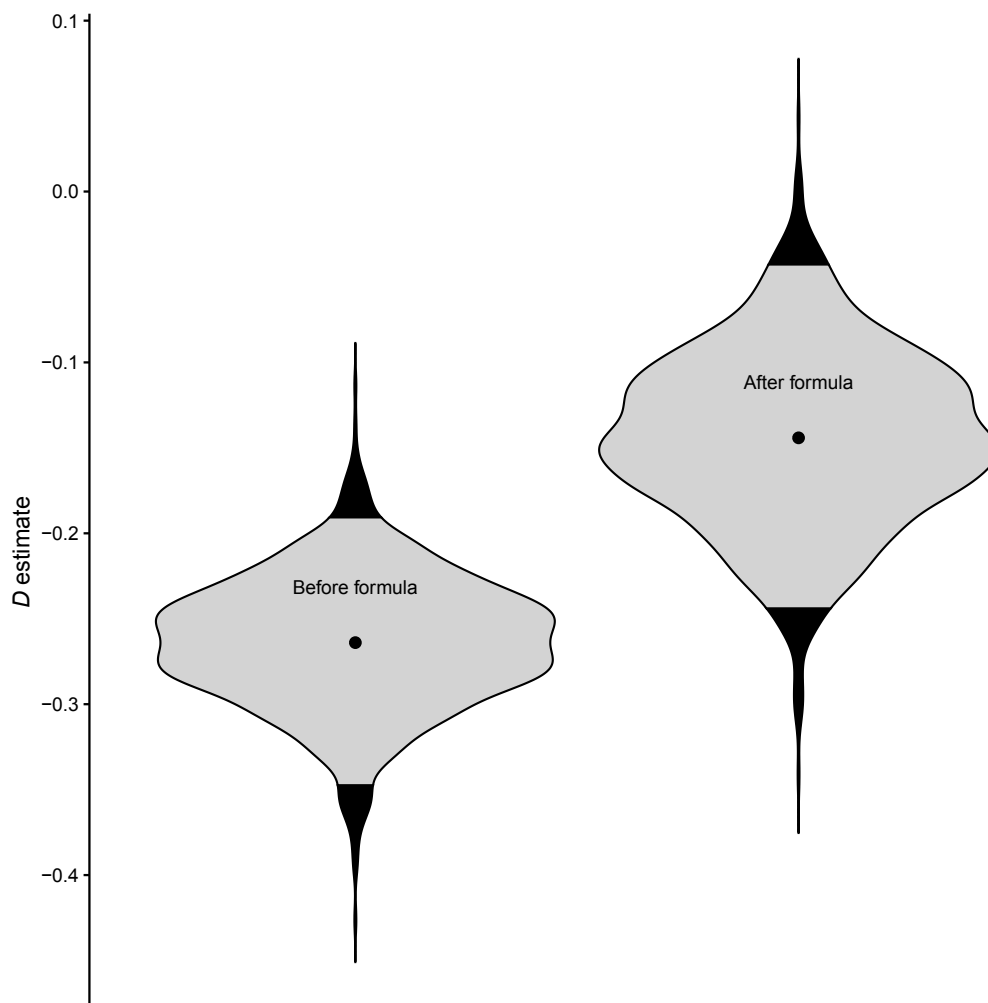
395 Dispersion parameter ( $D$ ) estimates for “moving pictures” [13] datasets. The subject’s sex is shown as the  
396 outline color of each violin, and the body site is shown as fill color. The four body sites for the female subject  
397 are shown at left, and the four body sites for the male subject are shown at right. Each violin shows the  
398 distribution of  $D$  estimates given by logistic error model bootstraps, and the dots within violins are means.  
399 Colored portions of violins represent 95% of bootstraps. The two subjects analyzed show parallel  $D$  estimates,  
400 with feces being the lowest, followed by palms which are all similar, followed by tongue communities. For  
401 both subjects, tongue patterns were not significantly different than the neutral model.

402 **Fig. 3**



403 Empirical phylodiversity accumulation in the infant gut microbiome [7]. Phylodiversity increases sharply after  
404 day 161 of the infant's life, then plateaus. This timing coincides with the day the subject began consuming  
405 baby formula. The times of sampling points are shown as vertical blue lines below the X-axis.

406 **Fig. 4**



407 Dispersion parameter ( $D$ ) estimates in the infant gut, pre-formula and during formula use. Formula use began  
408 on day 161, thus the first 160 days of the subject's life were analyzed separately. Community assembly was  
409 significantly underdispersed in the pre-formula dataset, but was not significantly different from the neutral  
410 model during formula use ( $P = 0.107$ ).

## 411 References

- 412 [1] Palmer MA, Ambrose RF, Poff NL. Ecological Theory and Community Restoration Ecology. *Restoration*  
413 *Ecology*. 1997 dec;5(4):291–300.
- 414 [2] Temperton VM. *Assembly Rules and Restoration Ecology: Bridging the Gap Between Theory and*  
415 *Practice*. Island Press; 2004.
- 416 [3] Richards SA, Possingham HP, Tizard J. Optimal fire management for maintaining community diversity.  
417 *Ecological Applications*. 1999 aug;9(3):880–892.
- 418 [4] Bengtsson J, Nilsson SG, Franc A, Menozzi P. Biodiversity, disturbances, ecosystem function and  
419 management of European forests. *Forest Ecology and Management*. 2000 jun;132(1):39–50.
- 420 [5] O’Dwyer JP, Kembel SW, Green JL. Phylogenetic diversity theory sheds light on the structure of  
421 microbial communities. *PLoS computational biology*. 2012 jan;8(12):e1002832.
- 422 [6] Goberna M, Navarro-Cano JA, Valiente-Banuet A, García C, Verdú M. Abiotic stress tolerance and  
423 competition-related traits underlie phylogenetic clustering in soil bacterial communities. *Ecology letters*.  
424 2014 oct;17(10):1191–201.
- 425 [7] Koenig JE, Spor A, Scalfone N, Fricker AD, Stombaugh J, Knight R, et al. Succession of microbial  
426 consortia in the developing infant gut microbiome. *Proceedings of the National Academy of Sciences of*  
427 *the United States of America*. 2011 mar;108 Suppl(Supplement\_1):4578–85.
- 428 [8] Frank DN, Harpaz N, St Amand AL, Pace NR, Feldman RA, Boedeker EC. Molecular-phylogenetic  
429 characterization of microbial community imbalances in human inflammatory bowel diseases. *Proceedings*  
430 *of the National Academy of Sciences*. 2007;.
- 431 [9] David LA, Materna AC, Friedman J, Campos-Baptista MI, Blackburn MC, Perrotta A, et al. Host  
432 lifestyle affects human microbiota on daily timescales. *Genome biology*. 2014 jan;15(7):R89.
- 433 [10] Peterfreund GL, Vandivier LE, Sinha R, Marozsan AJ, Olson WC, Zhu J, et al. Succession in the  
434 gut microbiome following antibiotic and antibody therapies for *Clostridium difficile*. *PloS one*. 2012  
435 jan;7(10):e46966.
- 436 [11] Kennedy RC, Fling RR, Robeson MS, Saxton AM, Donnell RL, Darcy JL, et al. Temporal Development  
437 of Gut Microbiota in Triclocarban Exposed Pregnant and Neonatal Rats. *Scientific reports*. 2016;6:33430.
- 438 [12] Guittar J, Shade A, Litchman E. Trait-based community assembly and succession of the infant gut  
439 microbiome. *Nature Communications*. 2019;.
- 440 [13] Caporaso JG, Lauber CL, Costello EK, Berg-Lyons D, Gonzalez A, Stombaugh J, et al. Moving pictures  
441 of the human microbiome. *Genome biology*. 2011 jan;12(5):R50.
- 442 [14] Nemergut DR, Schmidt SK, Fukami T, O’Neill SP, Bilinski TM, Stanish LF, et al. Patterns and  
443 processes of microbial community assembly. *Microbiology and molecular biology reviews : MMBR*. 2013  
444 sep;77(3):342–56.
- 445 [15] Nemergut DR, Knelman JE, Ferrenberg S, Bilinski T, Melbourne B, Jiang L, et al. Decreases in av-  
446 erage bacterial community rRNA operon copy number during succession. *The ISME Journal*. 2016  
447 may;10(5):1147–1156.
- 448 [16] Sprockett D, Fukami T, Relman DA. Role of priority effects in the early-life assembly of the gut micro-  
449 biota; 2018.
- 450 [17] Fukami T. Historical Contingency in Community Assembly: Integrating Niches, Species Pools, and  
451 Priority Effects. *Annual Review of Ecology, Evolution, and Systematics*. 2015;.
- 452 [18] Verster AJ, Borenstein E. Competitive lottery-based assembly of selected clades in the human gut  
453 microbiome. *Microbiome*. 2018;.

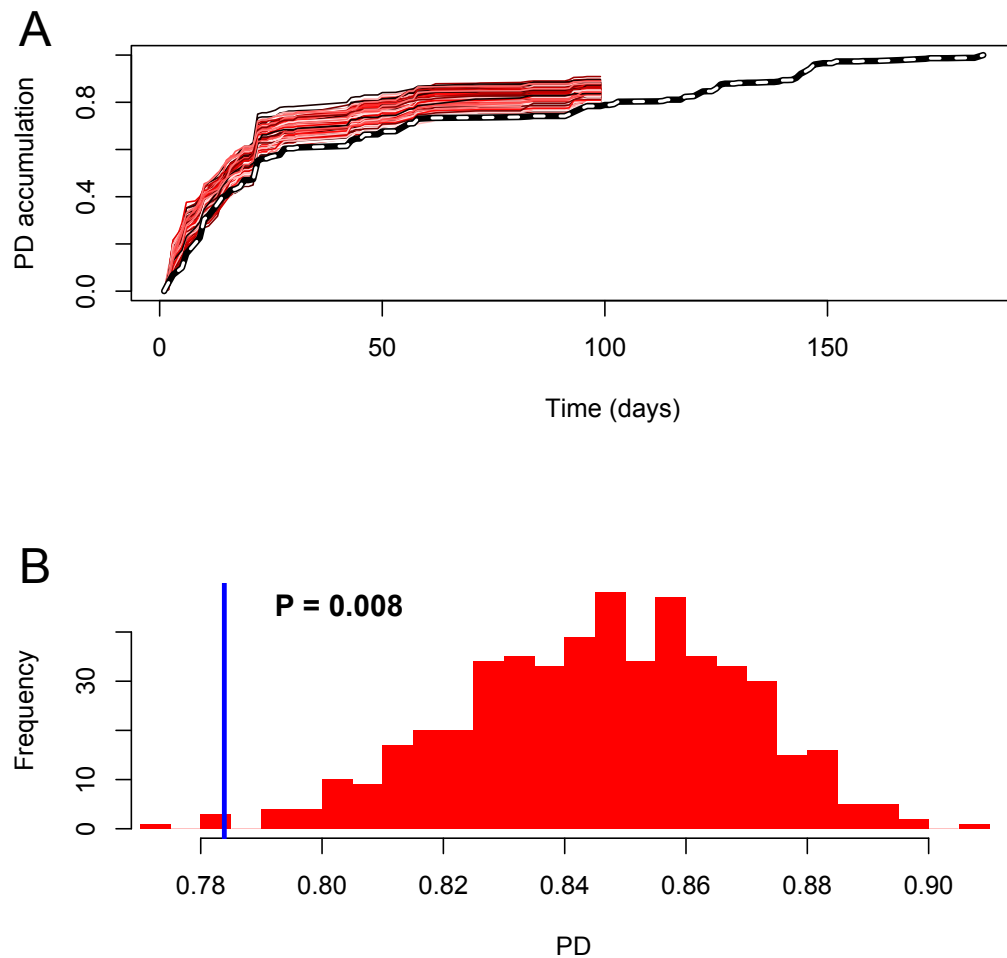
- 454 [19] Litvak Y, Bäumler AJ. The founder hypothesis: A basis for microbiota resistance, diversity in taxa  
455 carriage, and colonization resistance against pathogens. *PLoS Pathogens*. 2019 feb;15(2):e1007563.
- 456 [20] Zaneveld JR, Lozupone C, Gordon JJ, Knight R. Ribosomal RNA diversity predicts genome diversity  
457 in gut bacteria and their relatives. *Nucleic Acids Research*. 2010;38(12):3869–3879.
- 458 [21] Langille MGI, Zaneveld J, Caporaso JG, McDonald D, Knights D, Reyes JA, et al. Predictive functional  
459 profiling of microbial communities using 16S rRNA marker gene sequences. *Nature Biotechnology*. 2013  
460 aug;31(9):814–821.
- 461 [22] Losos JB. Phylogenetic niche conservatism, phylogenetic signal and the relationship between phylogenetic  
462 relatedness and ecological similarity among species; 2008.
- 463 [23] Darwin C. *On the Origin of Species*, 1859. London: Murray; 1859.
- 464 [24] Ma C, Li Sp, Pu Z, Tan J, Liu M, Zhou J, et al. Different effects of invader–native phylogenetic relatedness  
465 on invasion success and impact: a meta-analysis of Darwin’s naturalization hypothesis. *Proceedings of  
466 the Royal Society B: Biological Sciences*. 2016 sep;283(1838):20160663.
- 467 [25] Peay KG, Belisle M, Fukami T. Phylogenetic relatedness predicts priority effects in nectar yeast com-  
468 munities. *Proceedings of the Royal Society B: Biological Sciences*. 2012;.
- 469 [26] Li SS, Zhu A, Benes V, Costea PI, Hercog R, Hildebrand F, et al. Durable coexistence of donor and  
470 recipient strains after fecal microbiota transplantation. *Science (New York, NY)*. 2016 apr;352(6285):586–  
471 9.
- 472 [27] Tett A, Huang KD, Asnicar F, Fehlner-Peach H, Pasolli E, Karcher N, et al. The *Prevotella copri*  
473 complex comprises four distinct clades that are underrepresented in Westernised populations. *bioRxiv*.  
474 2019;.
- 475 [28] Stecher B, Chaffron S, Käppeli R, Hapfelmeier S, Friedrich S, Weber TC, et al. Like will to like:  
476 abundances of closely related species can predict susceptibility to intestinal colonization by pathogenic  
477 and commensal bacteria. *PLoS pathogens*. 2010 jan;6(1):e1000711.
- 478 [29] Brown CT, Xiong W, Olm MR, Thomas BC, Baker R, Firek B, et al. Hospitalized Premature Infants Are  
479 Colonized by Related Bacterial Strains with Distinct Proteomic Profiles. *mBio*. 2018 may;9(2):e00441–  
480 18.
- 481 [30] D’Andrea R, Riolo M, Ostling AM. Generalizing clusters of similar species as a signature of coexistence  
482 under competition”. *PloS Computational Biology*. 2019 jan;15(1).
- 483 [31] Webb CO, Ackerly DD, McPeck MA, Donoghue MJ. Phylogenies and Community Ecology. *Annual  
484 Review of Ecology and Systematics*. 2002 nov;33(1):475–505.
- 485 [32] Lozupone C, Knight R. UniFrac : a New Phylogenetic Method for Comparing Microbial Communities  
486 UniFrac : a New Phylogenetic Method for Comparing Microbial Communities. *Applied and environ-  
487 mental microbiology*. 2005;71(12):8228–8235.
- 488 [33] Washburne AD, Silverman JD, Leff JW, Bennett DJ, Darcy JL, Mukherjee S, et al. Phylogenetic  
489 factorization of compositional data yields lineage-level associations in microbiome datasets. *PeerJ*. 2017  
490 feb;5:e2969.
- 491 [34] Matsen FA, Evans SN, Gilks W, Ghodsi M, Kingsford C. Edge Principal Components and Squash  
492 Clustering: Using the Special Structure of Phylogenetic Placement Data for Sample Comparison. *PLoS  
493 ONE*. 2013 mar;8(3):e56859.
- 494 [35] Yassour M, Vatanen T, Siljander H, Hämäläinen AM, Härkönen T, Ryhänen SJ, et al. Natural history of  
495 the infant gut microbiome and impact of antibiotic treatment on bacterial strain diversity and stability.  
496 *Science Translational Medicine*. 2016;.

- 497 [36] Faith DP. Conservation evaluation and phylogenetic diversity. *Biological Conservation*. 1992 jan;61(1):1–  
498 10.
- 499 [37] Edgar RC. UNOISE2: improved error-correction for Illumina 16S and ITS amplicon sequencing. *bioRxiv*.  
500 2016; Available from: <http://www.biorxiv.org/content/early/2016/10/15/081257>.
- 501 [38] Martiny JBH, Jones SE, Lennon JT, Martiny AC. Microbiomes in light of traits: A phylogenetic  
502 perspective. *Science*. 2015 nov;350(6261):aac9323–aac9323.
- 503 [39] Vázquez-Baeza Y, Callewaert C, Debelius J, Hyde E, Marotz C, Morton JT, et al. Impacts of the Human  
504 Gut Microbiome on Therapeutics. *Annual Review of Pharmacology and Toxicology*. 2018;.
- 505 [40] Williamson BD, Hughes JP, Willis AD. A multi-view model for relative and absolute microbial  
506 abundances. *bioRxiv*. 2019; Available from: [https://www.biorxiv.org/content/early/2019/09/08/  
507 761486](https://www.biorxiv.org/content/early/2019/09/08/761486).
- 508 [41] Mayfield MM, Levine JM. Opposing effects of competitive exclusion on the phylogenetic structure of  
509 communities. *Ecology Letters*. 2010;.
- 510 [42] Wiens JJ, Ackerly DD, Allen AP, Anacker BL, Buckley LB, Cornell HV, et al. Niche conservatism as  
511 an emerging principle in ecology and conservation biology. *Ecology Letters*. 2010 oct;13(10):1310–1324.
- 512 [43] Scheffer M, van Nes EH. Self-organized similarity, the evolutionary emergence of groups of similar  
513 species. *Proceedings of the National Academy of Sciences*. 2006;103(16):6230–6235. Available from:  
514 <https://www.pnas.org/content/103/16/6230>.
- 515 [44] Webb CO. Exploring the Phylogenetic Structure of Ecological Communities: An Example for Rain  
516 Forest Trees. *The American naturalist*. 2000 aug;156(2):145–155.
- 517 [45] Cavender-Bares J, Ackerly DD, Baum DA, Bazzaz FA. Phylogenetic Overdispersion in Floridian Oak  
518 Communities. *The American Naturalist*. 2004;.
- 519 [46] Gerhold P, Cahill JF, Winter M, Bartish IV, Prinzing A. Phylogenetic patterns are not proxies of  
520 community assembly mechanisms (they are far better). *Functional Ecology*. 2015 may;29(5):600–614.
- 521 [47] Hubbell SP. *The Unified Neutral Theory of Biodiversity and Biogeography (MPB-32)*. Princeton Uni-  
522 versity Press; 2001.
- 523 [48] Emerson BC, Gillespie RG. Phylogenetic analysis of community assembly and structure over space and  
524 time. *Trends in ecology & evolution*. 2008 nov;23(11):619–30.
- 525 [49] Chatzidaki-Livanis M, Geva-Zatorsky N, Comstock LE. *Bacteroides fragilis* type VI secretion systems  
526 use novel effector and immunity proteins to antagonize human gut Bacteroidales species. *Proceedings  
527 of the National Academy of Sciences*. 2016;113(13):3627–3632.
- 528 [50] Hecht AL, Casterline BW, Earley ZM, Goo YA, Goodlett DR, Bubeck Wardenburg J. Strain competition  
529 restricts colonization of an enteric pathogen and prevents colitis. *EMBO reports*. 2016;17(9):1281–1291.
- 530 [51] Sakavara A, Tsirtsis G, Roelke DL, Mancy R, Spatharis S. Lumpy species coexistence arises robustly in  
531 fluctuating resource environments. *Proceedings of the National Academy of Sciences*. 2018;115(4):738–  
532 743. Available from: <https://www.pnas.org/content/115/4/738>.
- 533 [52] Morowitz MJ, Denev VJ, Costello EK, Thomas BC, Poroyko V, Relman DA, et al. Strain-resolved  
534 community genomic analysis of gut microbial colonization in a premature infant. *Proceedings of the  
535 National Academy of Sciences*. 2011;108(3):1128–1133.



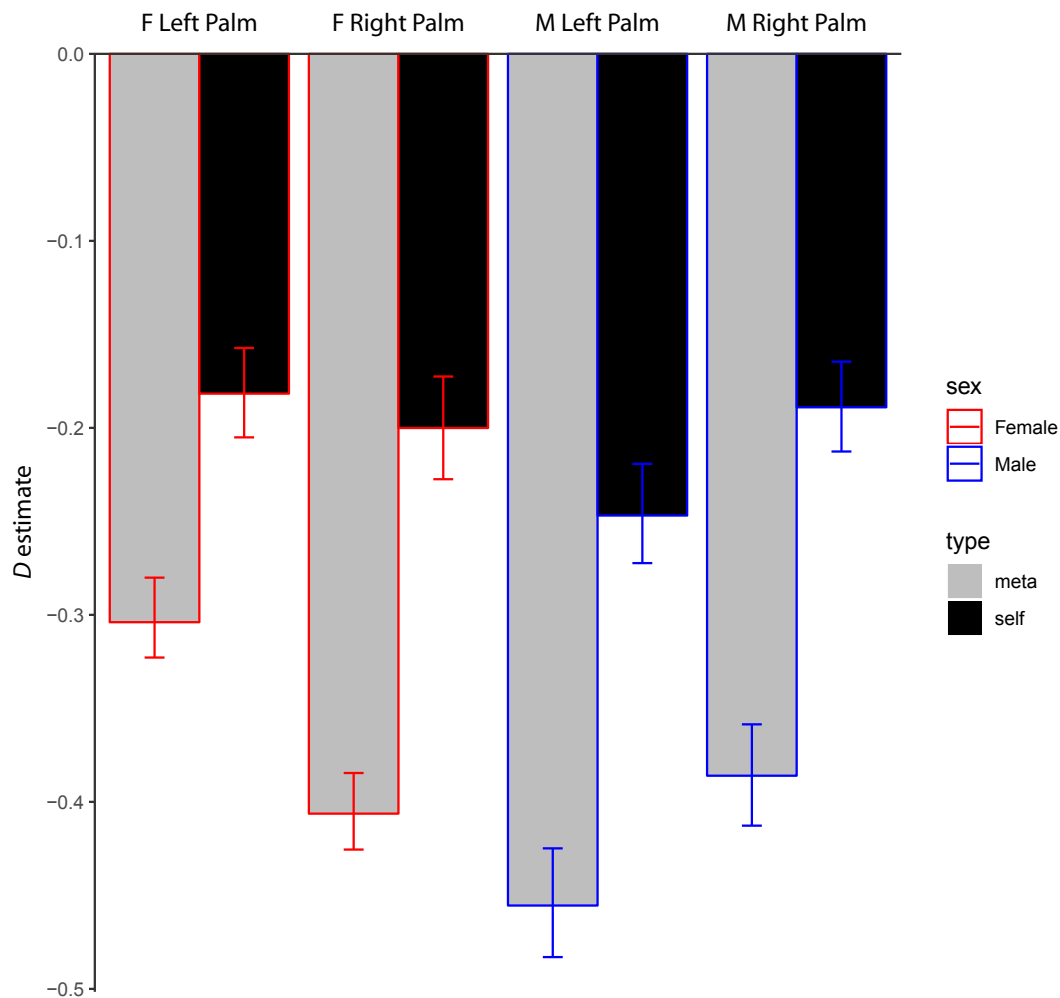
536 **Supplementary Material**

537 **Fig. S1**



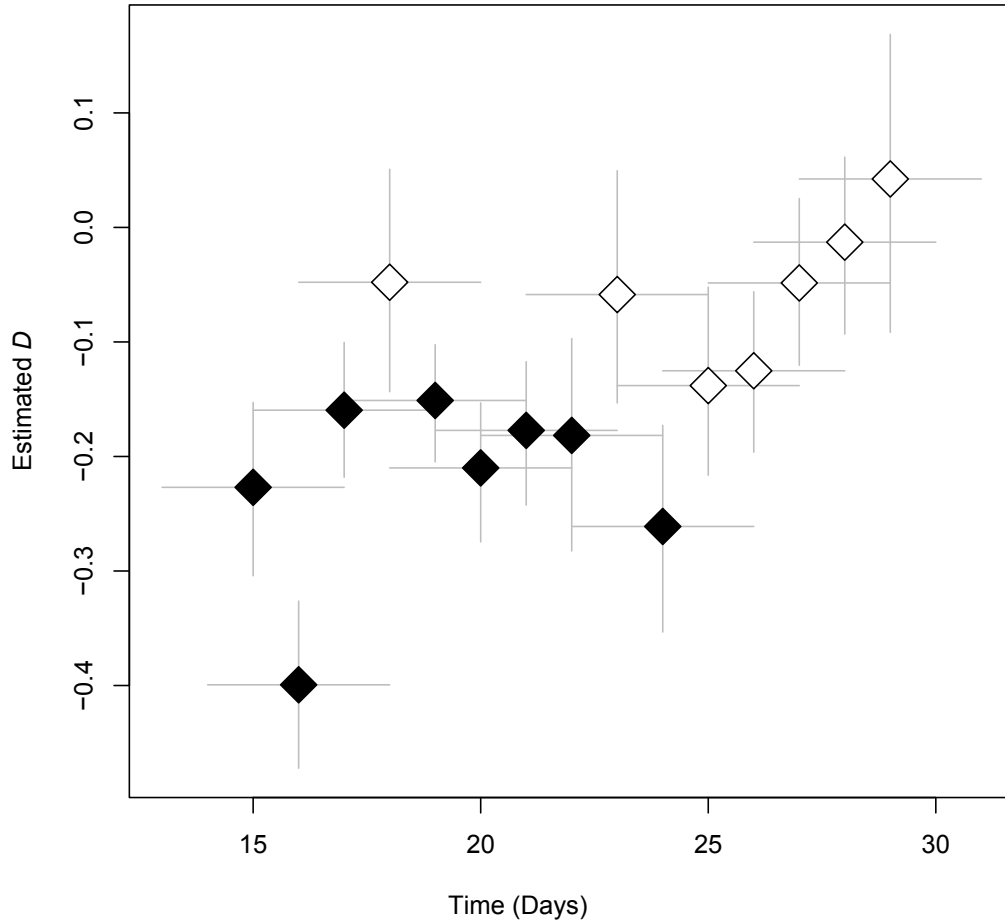
538 Significance testing for the female feces dataset. Plot A shows the empirical phylogenetic diversity accumulation  
539 (dashed; same as Fig. 1A) but with neutral model surrogate datasets shown in different shades of red.  
540 These are produced by running the neutral model 500 times, to generate a distribution of phylogenetic diversity  
541 values under  $D = 0$  (Plot B). As with all surrogate datasets, these are run until time  $m$  (see Parameter  
542 Estimation section of Materials and Methods). Empirical phylogenetic diversity at time  $m$  (blue line) is compared  
543 to the distribution of neutral model phylogenetic diversities at time  $m$  (red histogram), and a  $P$ -value is calculated  
544 as the proportion of neutral phylogenetic diversities more extreme than the empirical value.

545 **Fig. S2**



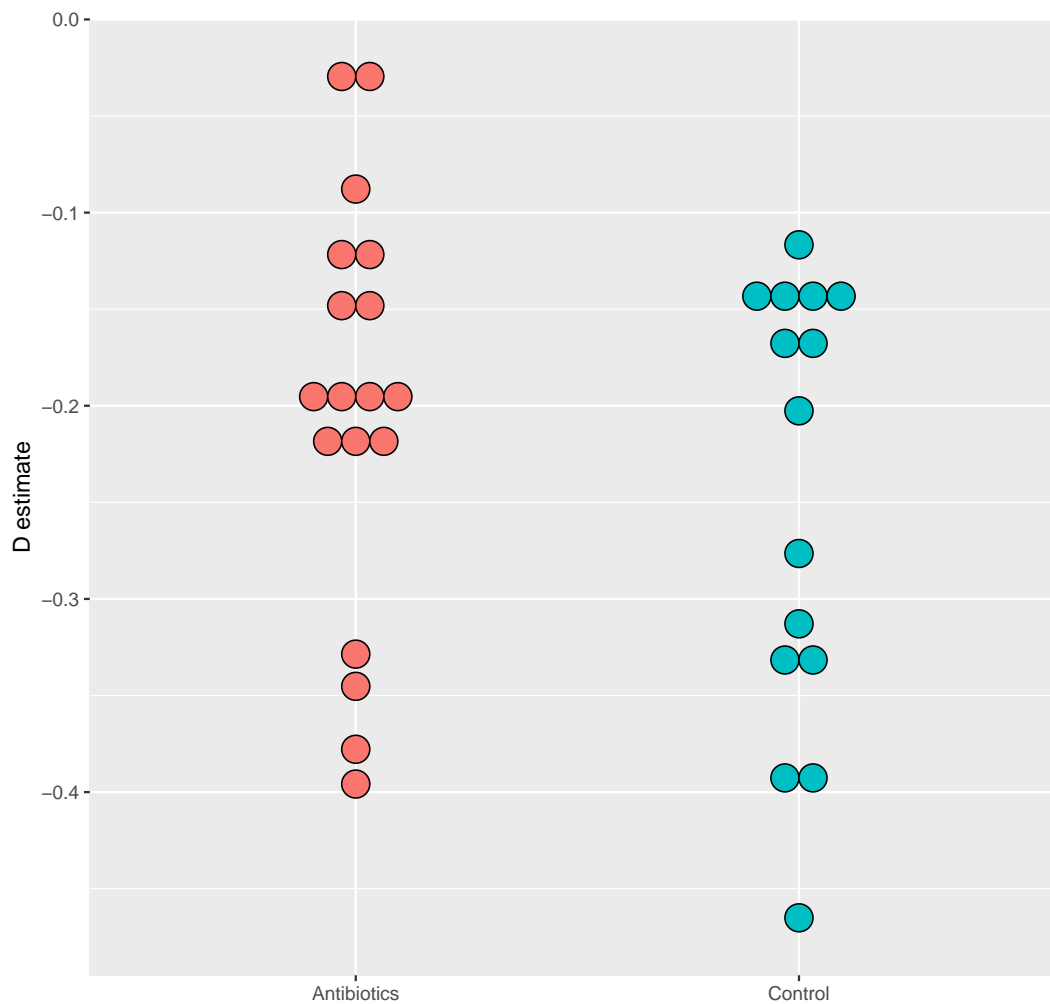
546 Comparison of “self” vs “meta” model results from palm communities. “Self” (black) models were run  
547 identically to Fig. 2), but “meta” (gray) models were run where the species pool for each palm community  
548 surrogate dataset was composed of all zOTUs observed across all four palm datasets. The difference between  
549 the “self”  $D$  estimate (generated above) and the “meta”  $D$  estimate (estimated with a metapopulation of  
550 zOTUs) is related to the exclusivity of recruitment into the community. In other words, if we were to estimate  
551 similar  $D$  values for both the “meta” and “self” analyses, the inclusion of extra species in the species pool  
552 would be of little importance to the model, and we would learn that it would make little difference to  
553 community assembly patterns if the species pool really was composed of the “meta” set.

554 **Fig. S3**



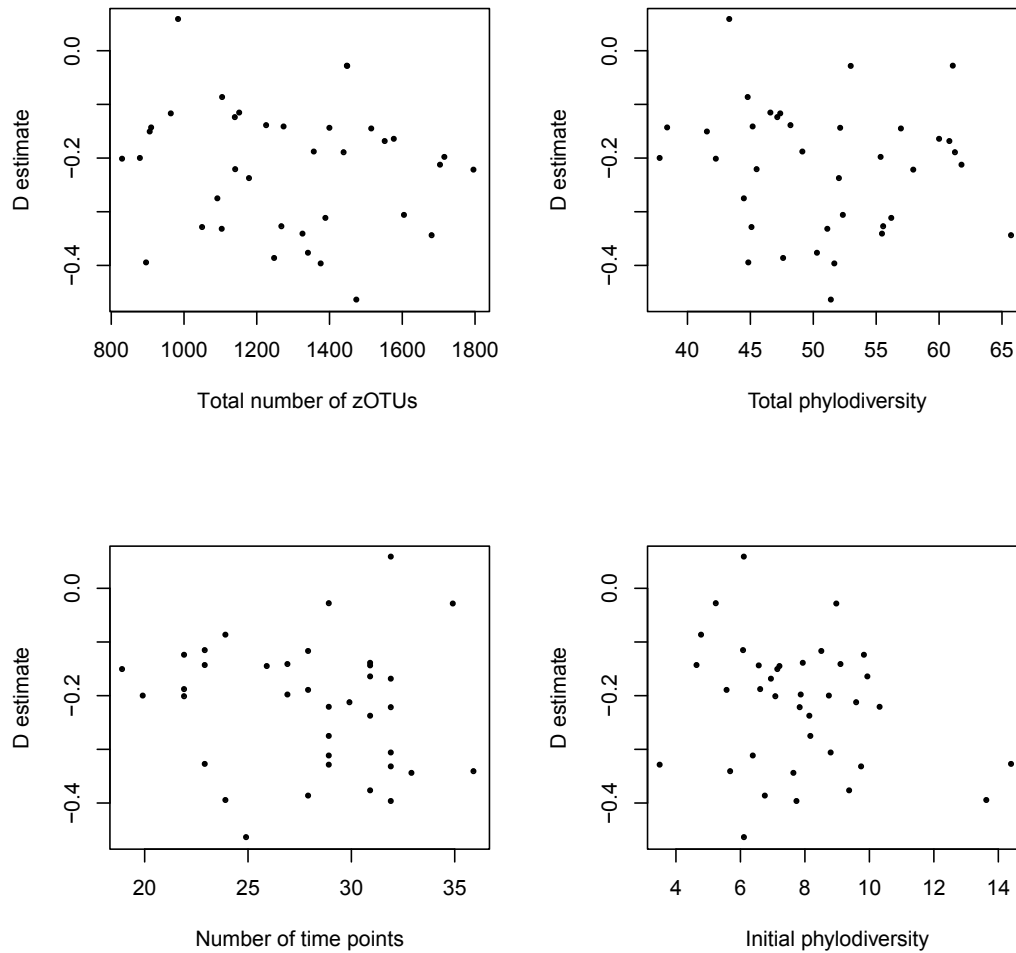
555 Sliding window analysis of male right palm data over 19 consecutive samples. We ran our model on each  
556 window of 5 continuous days (15 windows), in order to see how  $D$  varied over time. We only conducted this  
557 analysis for the section of samples that were sampled every day, so that comparisons between windows would  
558 not be confounded by window size. This analysis was done to demonstrate a potential use case for our model,  
559 and not to test any specific hypothesis. Filled shapes represent windows that were significantly different than  
560 the neutral model. Vertical bars represent 95% confidence intervals for  $D$  estimate, and horizontal bars  
561 represent window size.

562 **Fig. S4**



563 *D* estimates of Finnish infant datasets. All but two subjects exhibited significant phylogenetic underdis-  
564 persion. The two subjects that were not significantly different from the neutral model were both in the  
565 antibiotics cohort, which is comprised of infants that were treated with frequent antibiotics, almost all for  
566 ear infections. There was no significant difference between *D* values for the two groups.

567 **Fig. S5**



568 Relationship of  $D$  estimate to total zOTU richness, total phylodiversity, number of timepoints sampled, and  
569 initial phylodiversity (of first sample) for Finnish infant data. No statistically significant correlation was  
570 detected in any of these four analyses.